Fast Heating of Cylindrically Imploded Plasmas by Petawatt Laser Light

H. Nakamura,[1] Y. Sentoku,[2] T. Matsuoka,[3] K. Kondo,[1,3] M. Nakatsutsumi,[1] T. Norimatsu,[3] H. Shiraga,[3] K. A. Tanaka,[1,3] T. Yabuuchi,[1] and R. Kodama[1,3,4]

[1]*Graduate School of Engineering, Osaka University, Yamada-oka 2-1, Suita, Osaka, Japan*
[2]*Nevada Terawatt Facility, Department of Physics, MS-220, University of Nevada, Reno, Nevada 89557, USA*
[3]*Institute of Laser Engineering, Osaka University, Yamada-oka 2-6, Suita, Osaka, Japan*
[4]*CREST, Japan Science and Technology Agency, 5-Sanbancho, Chiyoda-ku, Tokyo, Japan*

(Received 15 January 2008; published 22 April 2008)

We produced cylindrically imploded plasmas, which have the same density-radius product of the imploded plasma ρR with the compressed core in the fast ignition experiment and demonstrated efficient fast heating of cylindrically imploded plasmas with an ultraintense laser light. The coupling efficiency from the laser to the imploded column was 14%–21%, implying strong collimation of energetic electrons over a distance of 300 μm of the plasma. Particle-in-cell simulation shows confinement of the energetic electrons by self-generated magnetic and electrostatic fields excited along the imploded plasmas, and the efficient fast heating in the compressed region.

DOI: 10.1103/PhysRevLett.100.165001 PACS numbers: 52.57.Kk, 52.40.Mj, 52.50.Gj

Development of ultraintense short pulse lasers has been opening new fields of science such as laser acceleration of electrons [1] and ions [2], and laser fusion, especially fast ignition approach in inertial fusion energy (IFE) research [3]. In the fast ignition scheme energetic electrons produced by an ultraintense laser heat a compressed high density imploded plasma. One of the methods that is advantageous to realizing efficient fast heating of the imploded plasma for the fast ignition is using a metal cone to guide an ultraintense laser light to the imploded plasma [4]. Efficient fast heating was demonstrated in the experiments using a spherical deuterated polystyrene shell target attaching a hollow gold cone [5]. Imploded plasmas were heated to an ion temperature of 0.8–1.0 keV and neutron yields with a 0.5 PW (1 PW $= 10^{15}$ W) laser heating were 1000 times greater than that without the PW laser heating.

Theoretical approaches have been made to understand the transfer of energy from the energetic electrons to the imploded plasmas. The mechanisms are still debated [6]. We need to elucidate the propagation of the energetic electrons in high temperature and high density plasmas to understand the mechanism of the fast heating of the imploded plasmas. Many experimental researches in the propagation of the energetic electrons were carried out [4,7]. Recently, we carried out guiding and collimation of the energetic electrons using a solid fine wire attached on a cone tip [7]. Because of results of these experiments, conductivity and magnetic and electric fields influenced on the propagation of energetic electrons. However, the conductivity and density gradient of imploded plasmas are clearly different from those of the solid wire. Therefore, in order to investigate the fast heating of the imploded plasmas, we need to use cylindrically imploded plasmas whose shape is similar to that of solid wire targets.

In this Letter, we report the first investigation of heating of cylindrically imploded plasmas with energetic electrons using a cone attached cylinder shell target. The energy coupling efficiency from the laser to the core plasma depends on the plasma density ρ, the stopping power of the energetic electrons, and the length L of the plasma along the propagation direction of energetic electrons. If plasmas have the same ρL as each other, the difference in the energy coupling depends on the propagation length in the imploded plasmas. Energy coupling and heating efficiency were estimated in the cylindrically imploded plasma as compared with the spherically imploded plasmas at the similar ρL. The experimental results are well consistent with two-dimensional particle-in-cell (PIC) simulation with PICLS-2D code indicating the collimation of the electrons in the cylindrical plasmas and efficient heating of the plasmas.

To create a long cylindrically imploded plasma, we used a cylindrical shell target attached two gold cones as shown in Fig. 1(a). The cylindrical shell consisted of CH layer (outer) and CD layer (inner), whose thickness was 2 and 5 μm, respectively. The diameter and the length of the shell were 400 μm and 1.2 mm, respectively. Two gold cone targets with open angles of 30° and 60° were attached at each side of the shell. The thickness of cone wall was 10 μm and the size of tip 50 μm. The distance between two cone tips was 500 μm.

Experiments were carried out using the GXII laser system at Osaka University, which has a short pulse laser (PW laser) and long pulse lasers [8]. Six beams of the long pulse lasers were used to implode the cylindrical hollow shell target. The energy of the one beam of the long pulse laser was 200 J, the duration of Gaussian-shaped pulse 1.2 ns (FWHM) and the wavelength 527 nm. The spot size was 500 μm and the intensity about 10^{13} W/cm^2 for each spot. Six beams illuminated the surface of the cylindrical shell with cylindrical symmetry as shown in Fig. 1(b). The PW laser was injected into the entrant cone for the heating of the imploded plasma. The energy was 120 J, the wavelength 1.053 μm, and the pulse duration between 0.7 and

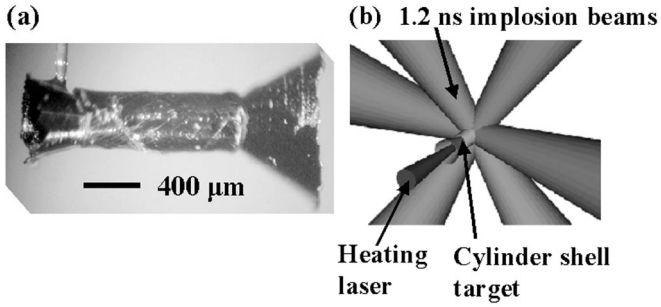

FIG. 1. (a) Cylindrical shell targets attached two gold cones. (b) Geometry of the implosion with six long pulse lasers and the heating laser.

1.1 ps. The spot size was 40–60 μm and the intensity about 10^{19} W/cm^2.

Figure 2(a) shows a typical time-integrated x-ray image of the cylindrically imploded plasma observed with a x-ray pinhole camera (XPHC) without the PW laser heating. The diameter was 30 ± 10 μm and the length 330 ± 10 μm, according to the x-ray profile of the image. Figure 2(b) shows an implosion dynamics of the cylindrical hollow shell. The squares represent the data points of the x-ray peak intensity from the imploded plasma vs the time observed with a x-ray streak camera (XSC) and the lines are radius-time trajectories calculated by ILESTA-1D simulation code [9]. The measured data were essentially consistent with the calculated data. Time = 0 represents the peak timing of the pulse. The timing of maximum compression was 1.25 ns from the peak timing of the pulse. The average density of the imploded plasma is 5.8–8.8 g/cm^3 and the average temperature 200 eV from the simulation. The ρL of the cylindrically imploded plasma will be 0.18–0.29 g/cm^2.

The PW laser illuminated the tip of the cone with an open angle of 30° at the maximum compression of the shell. The illumination timing of the PW laser was 1.25 ± 0.1 ns corresponding to the maximum compression from the XSC. In order to diagnose the heating temperature of the imploded plasma, we observed neutron spectra using a multichannel wave coincidence method to suppress the effect of gamma-ray signals and beamlike fusion neutron signals [10]. Four scintillation detectors were placed at distances of 2.5 and 3.5 m from the target and at angles of 46° and 138° relative to the direction of propagation of the PW laser beam. The time resolution of the detectors is 2.4–2.6 ns. Neutrons were generated by the fusion of two deuterium nuclei to a ^{3}He nucleus [$d(d, n)^3$He] in the imploded plasma. Figure 3 shows the D-D fusion neutron spectrum. Three peaks of the neutron appeared at energies of 2.25, 2.45, and 2.65 MeV in the spectrum. The neutrons at energies of 2.25 and 2.65 MeV were produced by the beamlike fusion reactions. These neutrons were symmetrically produced backward and forward, suggesting deuterium ions were radially accelerated. In contrast, peak at an energy of 2.45 MeV correspond to the neutrons from a

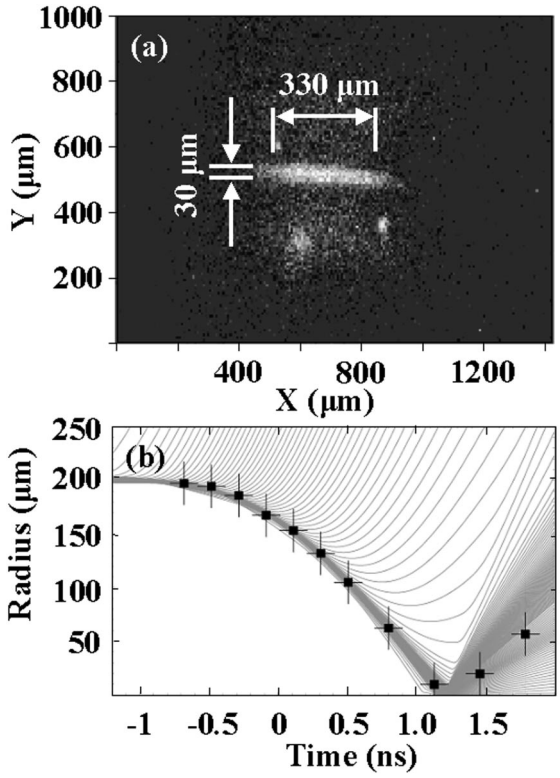

FIG. 2. (a) A typical x-ray time-integrated image of the cylindrical core plasma observed with the XPHC. The diameter of the cylindrical core plasma was 30 μm. The length along the laser axis was 330 μm. (b) Implosion dynamics of the cylindrical hollow shell. (Square) The data points of the peak intensity of the x-ray emission from the imploded plasma against the time observed with the XSC and (line) radius-time trajectories calculated by the ILESTA-1D simulation code.

thermonuclear reaction. The thermal neutron yields was enhanced to be $(2 \pm 1) \times 10^5$ by injection of the heating pulse. Without the PW laser heating, a D-D fusion thermal neutron signal was less than the detection limit of the diagnostics. Therefore neutron yields could be less than 10^4. The thermal neutron yields with the PW laser heating were more 10 times greater than the yields without the PW laser heating.

Thermal neutron spectra provide estimation of the plasma ion temperature. The plasma ion temperature is estimated using the relation of $T_i(\mathrm{keV}) = [\Delta E_{\mathrm{FWHM}}(\mathrm{keV})/c]^2$ [11], where ΔE_{FWHM} is the energy spread of thermal neutrons and $c = 82.48$ for deuterium-deuterium fusion reactions. The line in Fig. 3 is a Gaussian fit to the data points, indicating the spectral width of 119 keV. Taking account of the energy resolution of the detectors, this spectral width is corresponding to (600 ± 50) eV for the plasma ion temperature. The efficiency of an energy coupling of the PW laser to the imploded plasma is estimated from the heated volume and the heating temperature. The coupling energy E_c is calculated using equation of $E_c = [\Delta T(\mathrm{eV})]V\rho(1 + Z)e$, where ΔT(eV), V, and ρ represent an increase in an ion temperature, volume of a

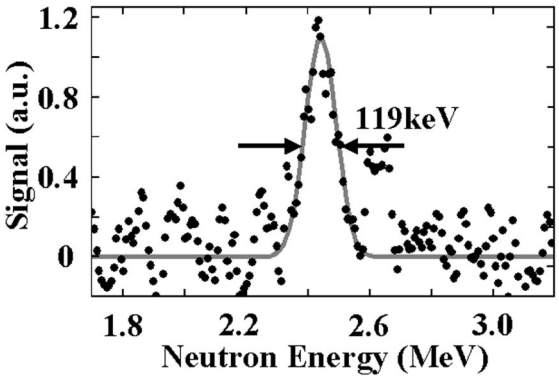

FIG. 3. A thermal neutron spectrum. Thermal neutron yields were $(2 \pm 1) \times 10^5$. The line is a Gaussian fit to the data points, indicating a spectral width of 119 keV.

imploded plasma, and density of the imploded plasmas. The calculated coupling energy could be 18–27 J, which was indicating the efficiency η_c could be 14%–21%.

The coupling efficiency of the energy for the cylindrically imploded plasma is compared to that for the spherical imploded plasma, indicating the propagation of the energetic electrons in the imploded plasma. In the experiments of the spherical imploded plasma [4,5], the density of the imploded plasma was 50–70 g/cm^3 the volume $45 \times 40 \times 40$ μm^3 and the ρL of the plasma 0.20–0.32 g/cm^2. In the heating process, the coupling efficiency of the energy from the PW laser to the spherical imploded plasma was $\eta_s =$ 15%–30% (Table I). On the other hand, the ρL of the cylindrically imploded plasma is 0.18–0.29 g/cm^2, which is comparable to that for the spherical plasmas. Hereby, the distance of propagation of the energetic electrons in the imploded plasma is estimated without absolute value of the stopping power in the imploded plasmas. The efficiency η depend on effects of the divergence of electron beams and the stopping power of the imploded plasmas, which is related to ρL. Efficiency η_θ due to the effect of divergence of the energetic electrons is expressed as a ratio of the volume of the imploded plasma to the region where diverged electron beams propagate. If the electron beams propagated with collimation in the imploded plasmas, the efficiency of energy coupling would be $\eta_c = 13\%$–27%, using $\eta_c = (\rho L_c/\rho L_s)\eta_s$, where the subscripts "$c$" and "$s$" represented cylindrical and spherical, respectively. On the other hand, if the energetic electrons propagated with a divergence between 20° and 40°, the efficiency η_c might be 2%–7%, using $\eta_c = (\eta_{\theta_c}/\eta_{\theta_s})(\rho L_c/\rho L_s)\eta_s$. The energetic electrons could propagate with collimation in the imploded plasma according to the experimental results.

A two-dimensional PIC simulation code [12] is used to clarify the physics mechanism associated with the collimation. The cone target and the imploded column plasma are modeled. The plasma parameters as an initial condition in the simulation are based upon the results from the hydrodynamics simulations. The cylindrically imploded plasma has an exponential radial profile and the peak density is 8000 times as large as the critical density n_c. The imploded plasma has initial electron and ion temperatures of 150 eV. The initial density profile of the cylindrically imploded plasma is plotted as contour lines in Fig. 4(c). The density of a cone target is $500n_c$. Note here that since the cone target is modeled by low-Z plasma, the energetic electrons scattered inside the cone target is underestimated by the simulation. The laser pulse consists of a half-Gaussian pulse of 150 fs as a rise time and is kept constant after 150 fs for 1 ps. The maximum of the normalized vector potential is $a = 3.75$ ($\equiv eA/m_e c^2$), which corresponds to $I_0 = 2 \times 10^{19}$ W/cm^2.

The results of the PIC simulation show the generation of magnetic and electric fields around the cylindrically imploded plasma in an area of a critical density as shown in Figs. 4(a) and 4(b) at $t = 460$ fs. The radial electric field and the azimuthal magnetic field are created around the region of the critical density along the cylindrically imploded plasmas. The front of these fields propagate along the cylinder with the energetic electrons at almost the light velocity. The radial expansions of these fields are ignored while the energetic electrons propagate in the cylindrical plasmas. Escaped electrons moving radially from the imploded plasmas create electrical sheath fields. The propagations of the energetic electrons and the gradients of the electron current density create the magnetic fields. The mechanism of generation of these fields is similar to that with solid wire targets [7]. However, the magnitude of the fields with the cylindrically imploded plasmas is smaller than that with the solid wire. The magnitude of the magnetic fields is ±50 MG and electric fields ±1.5 TV/m at $t = 460$ fs. Increasing of the density gradient of the cylindrically imploded plasma compared with that of the solid wire target reduces the electric field. Decreasing of the

TABLE I. Comparison of parameters of imploded plasmas and the experimental results of neutron measurements.

Parameter	Cylindrical	Spherical
Size	$330 \times 30 \times 30$ μm^3	$45 \times 40 \times 40$ μm^3
Density	5.5–8.8 g/cm^3	50–70 g/cm^3
ρL	0.18–0.29 g/cm^2	0.20–0.32 g/cm^2
Neutron yield	2×10^5	$2 \times^5$ 10–1×10^7
Heated temperature	0.6 keV	0.8–1.0 keV
Efficiency of energy coupling	14%–21%	15%–30%

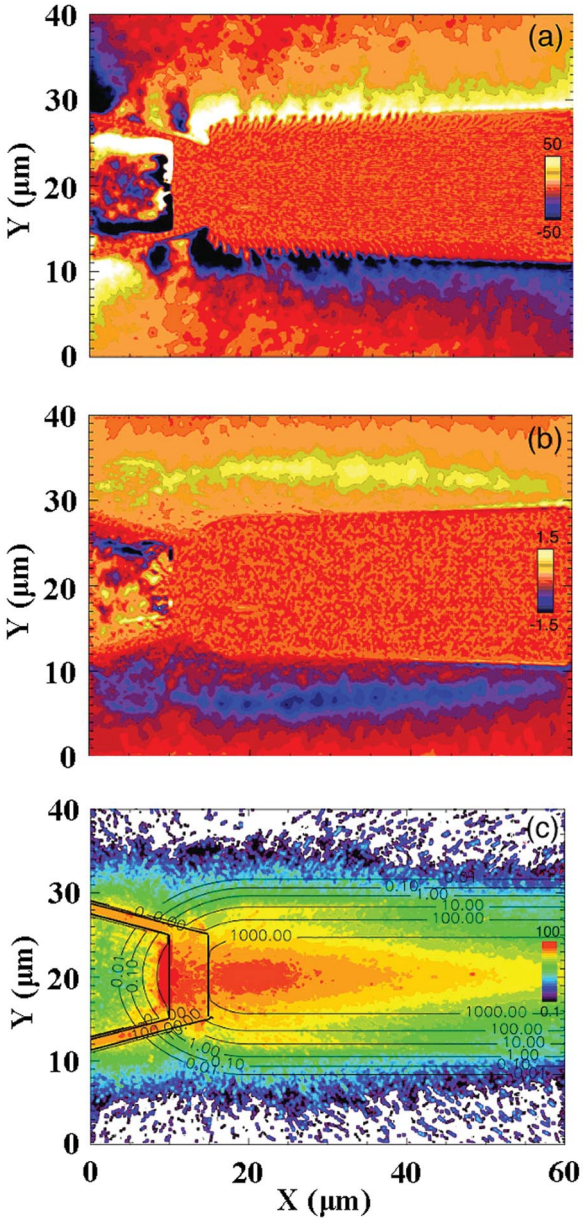

FIG. 4 (color). Contours of (a) magnetic field and (b) electric field around the cylindrical plasma at $t = 460$ fs from two-dimensional PIC simulation. The magnitude of magnetic field is ± 50 MG and the magnitude of electric field is ± 1.5 TV/m. (c) Contours of electron energy density at $t = 460$ fs.

diameter of the plasmas reduces the magnetic field because of decreasing the current density gradient of the energetic electrons. In the magnetic fields, which is more than 50 MG, Larmor radius R_L is less than a few μm for the electrons $\epsilon_K \leq 10$ MeV, taking into account a relativistic effect γ. The energetic electrons, which are going out from the imploded region, are trapped by the magnetic fields and no energy transport to the outer region as seen in Fig. 4(c). At the same time those energetic electrons are pulled back into the imploded region by the electrostatic field similar to a drift motion in plasmas into the region of the dense plasma. On the other hand, the fields are not driven in the region of higher density than solid density. Thereby, the energetic electrons can propagate in the cylindrically imploded plasma and deposit the energy in the high density region through the collisional processes as seen in Fig. 4(c) [13]. The average electron energy at the center of the column plasma drops exponentially. It is about a few keV behind the cone tip and 400 eV at $X = 60$ μm at $t = 460$ fs.

In conclusion, fast heating of the cylindrically imploded plasmas was demonstrated with cone attached cylinder shell targets. The energy coupling efficiency from the PW laser to the imploded plasmas was 10%–20%, implying that the propagations of the energetic electrons could be collimated in a distance of 300 μm of the imploded plasma. Particle-in-cell simulation shows that the energetic electrons are trapped in the magnetic field surrounding the imploded plasmas with a scale of a few μm of the Larmor radius and are pulled back by an electrostatic field into the dense region, resulting the collimation of the energetic electrons and the efficient fast heating.

The authors would like to thank the technical staff at the Institute of Laser Engineering for their support in operation of the laser system operation, target fabrication, and data acquisition. Simulation work was supported by UNR under DOE/NNSA Grant No. DE-FC52-06NA27616.

[1] S. C. Wilks, W. L. Kruer, M. Tabak, and A. B. Langdon, Phys. Rev. Lett. **69**, 1383 (1992); M. H. Key *et al.*, Phys. Plasmas **5**, 1966 (1998).
[2] L. Robson *et al.*, Nature Phys. **3**, 58 (2007); J. Fuchs *et al.*, Nature Phys. **2**, 48 (2006).
[3] M. Tabak *et al.*, Phys. Plasmas **1**, 1626 (1994).
[4] R. Kodama *et al.*, Nature (London) **412**, 798 (2001).
[5] R. Kodama *et al.*, Nature (London) **418**, 933 (2002).
[6] R. B. Campbell, R. Kodama, T. A. Mehlhorn, K. A. Tanaka, and D. R. Welch, Phys. Rev. Lett. **94**, 055001 (2005); R. J. Mason, Phys. Rev. Lett. **96**, 035001 (2006).
[7] R. Kodama *et al.*, Nature (London) **432**, 1005 (2004); Z. L. Chen *et al.*, Phys. Rev. Lett. **96**, 084802 (2006).
[8] Y. Kitagawa *et al.*, IEEE J. Quantum Electron. **40**, 281 (2004).
[9] H. Takabe *et al.*, Phys. Fluids **31**, 2884 (1988).
[10] H. Nakamura *et al.*, Rev. Sci. Instrum. **77**, 10E727 (2006).
[11] H. Brysk, Plasma Phys. **15**, 611 (1973).
[12] Y. Sentoku and A. J. Kemp, J. Comput. Phys. (to be published).
[13] A. J. Kemp, Y. Sentoku, V. Sotnikov, and S. C. Wilks, Phys. Rev. Lett. **97**, 235001 (2006).